Research Article

Journal of Environmental Nanotechnology

Behavior of High-performance Geopolymer Concrete Beams with Substitution of Silica Fume and GGBS/Fly Ash

A. Kandasamy[1*], B. Ramesh[1], Mahmoud Al Khazaleh[2] and K. Athiappan[3]

[1]Department of Civil Engineering, Saveetha School of Engineering, Saveetha University, Chennai, TN, India
[2]Department of Civil Engineering, Dean of Munib and Angela Masri Faculty of Engineering, Aqaba University of Technology, Aqaba, Jordan
[3]Department of Civil Engineering, Thiagarajar College of Engineering, Madurai, TN, India
Received: 03.01.2025 Accepted: 23.03.2025 Published: 30.03.2025
*asohankandasamy@gmail.com

ABSTRACT

The flexural behaviour of high-performance geopolymer concrete (HPGPC) beams with partially substituted ground granulated blast furnace slag (GGBS)/fly ash and silica fume (SF) is examined in this experimental investigation. An alkaline activator solution consisting of sodium hydroxide and sodium silicate in a 1:1.5 ratio at 8M concentration was used to create geopolymer concrete in place of traditional cement. Seven distinct mix proportions (M1–M7) were made with variable amounts of SF replacement (0%, 5%, 7.5%, and 10%), and in certain mixes, a continuous 0.2% glass fibre reinforcement was added. The concrete mix was intended to reach a goal mean strength of 80 MPa. Mechanical attributes such as modulus of elasticity, water absorption, flexural strength, split tensile strength, and compressive strength were assessed. According to the findings, 7.5% silica fume replacement is ideal for increasing compressive strength, and 0.2% glass fibre addition further boosts tensile and flexural performance. Seven 100 × 200 × 2000 mm geopolymer concrete beams were also cast, allowed to cure for 28 days, and then tested under two-point loading in a loading frame with a 1000 kN capacity. Important flexural parameters were examined, including moment-curvature, moment-rotation characteristics, deflection, ultimate load, and first fracture load. Evaluations comparing high-performance geopolymer concrete beams to control specimens showed improved ductility and load-bearing capability, demonstrating the efficiency of glass fibre and silica fume in maximizing flexural behaviour.

Keywords: Geopolymer concrete; Silica fume replacement; Glass fiber reinforcement; High-performance concrete

1. INTRODUCTION

Geopolymer concrete (GPC) is an eco-friendly alternative to traditional cement-based concrete, offering reduced carbon emissions and enhanced mechanical properties. The use of supplementary materials like silica fume (SF) and ground granulated blast furnace slag (GGBS) improves its strength and durability. Incorporating glass fiber reinforcement further enhances flexural performance, making it suitable for high-performance structural applications. This study investigates the influence of SF replacement and fiber addition on the mechanical and flexural behavior of GPC beams.

A recent research (Tashan, 2022) on high performance geopolymer concrete (HPGPC) beams showed enhanced flexural behaviour and ductility when silica fume and GGBS/fly ash were partially substituted. Additionally, studies show that mended HPGPC beams maintain their strength and that new fissures develop rather than reopen, guaranteeing structural endurance. Prakash *et al.* (2021) studied silica fume and GGBS/fly ash-incorporated HPGPC beams. They demonstrated their improved durability and mechanical strength. According to studies, optimal replacement levels enhance flexural and compressive performance, and their combined effects result in better structural behavior. Thakur *et al.* (2022) studied HPGPC beams with partial silica fume and GGBS/fly ash replacement, which emphasized the role of alkali ratios and binder composition in optimizing mechanical properties. Research findings confirm that GGBS significantly enhances compressive and flexural strength, contributing to sustainable and durable concrete structures. Abdellatief *et al.* (2022) reported that ultra-high performance geopolymer mixes have improved early-age strength and durability. Additionally, geopolymer concrete was shown as a promisable sustainable substitute for conventional cement. By improving microstructural integrity *via* optimized silica fume and activator compositions, geopolymer concrete may be used in high-strength applications. Swathi and Vidjeapriya, (2023) used aluminosilicates to lessen environmental effect, and the geopolymer concrete became more popular as a sustainable substitute for conventional cement-based concrete. However, issues with strength, durability, and curing conditions still

prevent it from being widely used, requiring further research into high performance and ultra-high-performance blends. Sujitha *et al.* (2024a) reported that incorporating silane-functionalized halloysite nano clay (SNC) with sodium polyacrylamide (SAP) enhanced cementitious materials by improving hydration and filling microspores. This combination significantly increased compressive, flexural, and tensile strengths while reducing shrinkage and microcrack formation, making it suitable for durable concrete applications. Similarly, Sujitha *et al.* (2024b) highlighted that the use of silanized graphene oxide (SGO) with SAPs enhanced hydration, minimizes shrinkage, and improved water retention and durability in cement-based materials. The SGO/SAP composite contributed to high-performance concrete by promoting internal curing, strengthening the concrete matrix, and reducing microcracks. Geopolymer concrete produced through the polycondensation of aluminosilicate materials with alkaline activators, exhibited superior durability and mechanical properties while reducing CO_2 emissions (Nagajothi *et al.* 2022). This study indicated that geopolymer concrete demonstrated better resistance to acid attack, sulphate exposure, and water absorption compared to conventional concrete, making it a sustainable alternative for construction applications. Geopolymer recycled aggregate concrete (GRAC) developed using GGBS and fly ash, exhibited superior sulfate resistance and sustainability by eliminating cement usage (Xie *et al.* 2019). This work highlighted its reduced mass loss and higher residual compressive strength, making it a viable alternative for construction in sulfate-rich environments. High-strength geopolymer concrete incorporating GGBS, fly ash, and silica fume exhibited superior mechanical properties, surpassing target compressive, flexural, and tensile strengths (Hawarneh *et al.* 2024). This demonstrated its potential as a sustainable alternative to conventional concrete with enhanced durability and performance. Geopolymer concrete incorporating incinerated biomedical waste ash (IBWA) and glass powder offered a sustainable solution for waste utilization while enhancing concrete performance (Suresh *et al.* 2021). The combination of IBWA and GGBS improved reactivity, making it a viable alternative to conventional cement-based concrete. Geopolymer concrete with fly ash and GGBS showed promising potential as a sustainable alternative to pavement quality concrete, reducing CO_2 emissions and embodied energy (Rambabu *et al.* 2024). Its superior mechanical properties, lower shrinkage strain, and fatigue resistance made it suitable for medium-load traffic pavements. Saini *et al.* (2024) emphasized that natural fiber-based reinforcements in reinforced concrete (RC) offered a sustainable alternative to conventional materials. These reinforcements not only reduce carbon emissions but also enhanced mechanical properties, making them suitable for both new construction and retrofitting applications. Machine learning techniques are utilized to predict the compressive strength of geopolymer concrete, considering its complex mix design and material variability (Amin *et al.* 2022). This study has shown that ensemble learning approaches, particularly random forest and bagging methods, enhance prediction accuracy, making them effective tools for optimizing geopolymer concrete formulations.

Despite extensive research on geopolymer concrete, limited studies have investigated the combined effect of silica fume replacement and glass fiber reinforcement on high-performance geopolymer concrete beams. While existing studies primarily focus on compressive strength, a comprehensive analysis of flexural behavior, including moment-curvature and moment-rotation characteristics, remains unexplored. Additionally, most research emphasizes conventional curing methods, whereas this study examines the flexural performance of HPGPC beams under ambient conditions, making it more practical for real-world applications. Although silica fume is known to enhance microstructural integrity, its optimal replacement level for balancing compressive and flexural strength requires further investigation. Furthermore, the role of continuous glass fiber reinforcement in improving ductility and crack resistance in geopolymer concrete beams has not been widely studied. The novelty of this research lies in evaluating the structural efficiency of HPGPC beams incorporating silica fume and glass fiber under realistic loading conditions. Through an in-depth experimental approach, this study addresses the knowledge gap by providing insights into the synergistic effects of silica fume and glass fiber reinforcement, ultimately contributing to the advancement of sustainable and high-performance concrete materials.

2. MATERIALS AND METHODS

Table 1. Materials and specifications

Material	Specifications
Cement	OPC 43 Grade, IS: 12269 – 1987
Fine Aggregate	River sand, Grading Zone II, IS: 383 – 1970
Coarse Aggregate	Crushed blue granite, 20 mm, IS: 383 – 1970
Silica Fume (SF)	ELKEM India (P) Ltd., ASTMC 1240, Specific Gravity: 2.2
GGBS/Fly Ash	Industrial by-products used in geopolymer mix
Glass Fibers	Cem-Fil Anti Crack HD, Density: 2.6 t/m³, Tensile Strength: 1700 MPa
Alkaline Activator	NaOH & Na_2SiO_3 (1:1.5 ratio), 8M concentration
Super Plasticizer	CERAPLAST 300, improves workability & reduces W/C ratio
Water	Potable water

Table 1 shows the materials and specifications used in this study.

2.1 Experimental Methodology

2.1.1 Mixing Proportion Details

The concrete mixture followed ACI Committee standards to develop 80 MPa compressive strength. The experiment involved replacement of cement with silica fume at four different ratios ranging from 0% to 5% and 7.5% and ending at 10% while adding glass fibers to select combinations. Specially designed mix proportions protected workability coupled with strength and durability performance. The mix proportion information together with details appears in Table 2, Table 3 and Table 4.

2.1.2 Mix Design Calculation

The mix design was based on the absolute volume method, assuming an air content of 1%. The key components were calculated as follows:

Table 2. Mix proportions of admixtures in percentage

Mix	SF (kg/m³)	Glass Fiber (kg/m³)
M1	0	0
M2	30	0
M3	45	0
M4	60	0
M5	30	1.2
M6	45	1.2
M7	60	1.2

Table 3. Mix proportion ratios

Mix	SF (kg/m³)	Glass Fiber (kg/m³)	Ratio
M1	0	0	1:0.99:1.89:0.26
M2	30	0	1:0.99:1.89:0.26
M3	45	0	1:0.99:1.89:0.26
M4	60	0	1:0.99:1.89:0.26
M5	30	1.2	1:0.99:1.89:0.26
M6	45	1.2	1:0.99:1.89:0.26
M7	60	1.2	1:0.99:1.89:0.26

The methodology adopted in this research follows a systematic approach for designing and testing high-performance geopolymer concrete beams with partial replacement of silica fume (SF) and incorporation of glass fibers. Seven different mix proportions were prepared, with varying SF content (0%, 5%, 7.5%, and 10%) and glass fiber reinforcement (0.2% in select mixes). The mix design adhered to ACI committee recommendations and used the absolute volume method to proportion aggregates and binder content.

A w/b ratio of 0.26 was maintained for all mixes, ensuring workability and strength. The fine aggregate content was kept constant at 594 kg/m³, while the coarse aggregate content was 1134 kg/m³. Superplasticizer dosage was adjusted based on the binder content to enhance workability.

This optimized mix design was used to cast concrete beams (100 × 200 × 2000 mm), which were cured for 28 days before testing under a 1000 kN capacity loading frame. The methodology ensures an accurate assessment of the flexural behavior, mechanical properties, and durability of the high-performance geopolymer concrete beams, thereby validating the influence of silica fume and glass fibers on strength enhancement and structural performance.

Table 4. Mix proportion details

Mix	Cement (kg/m³)	Alkali Activated Materials (AAM)	SF (kg/m³)	Glass Fiber (kg/m³)	Superplasticizer (lit/m³)
M1	610	0	0	0	10.73 (2.2%)
M2	-	575	30	0	11.71 (2.4%)
M3	-	545	45	0	12.20 (2.5%)
M4	-	530	60	0	13.17 (2.7%)
M5	-	570	30	1.2	11.71 (2.4%)
M6	-	555	45	1.2	12.20 (2.5%)
M7	-	543	60	1.2	13.17 (2.7%)

3. EXPERIMENTAL WORK AND PROCEDURES

Testing related to workability and strength-based characteristics of high performance concrete containing silica fume and Cem-Fil anti crack fibers took place through experimental methods.

Steel moulds served as the casting material for all the test specimens, which included cubes and cylinders. The specimens were obtained from moulds after 24 hours and immersed in water for curing. The tests on cube specimens included compressive strength determination and water absorption measurements, whereas cylinder specimens provided results for split tensile strength along with flexural strength and modulus of elasticity data. The flexural testing and shear testing utilized beam specimens for analysis. Table 5 provides a list of apparatus specifications regarding test samples.

Table 5. Types of tests and specimen sizes

Mix	SF (kg/m³)	Glass Fiber (kg/m³)	28 Days MPa	Theoretical Value MPa
M1	0	0	5.23	5.83
M2	30	0	5.78	5.88
M3	45	0	5.97	6.09
M4	60	0	5.84	5.99
M5	30	1.2	6.12	5.88
M6	45	1.2	6.58	6.16
M7	60	1.2	6.35	6.05

Table 6. Compressive strength results

S. No	Property Tested	Sample Type	Quantity (No. of Samples)	Dimensions (mm)
1	Compressive Strength	Cube	105 (7 × 15)	100 × 100 × 100
2	Flexural Strength	Prism	21 (7 × 3)	100 × 100 × 500
3	Split Tensile Strength	Cylinder	21 (7 × 3)	100 × 200
4	Water Absorption	Cube	14 (7 × 2)	100 × 100 × 100
5	Modulus of Elasticity	Cylinder	14 (7 × 2)	100 × 200
6	Flexural Behavior	Beam	7 (7 × 1)	100 × 200 × 2000

3.1 Compressive Strength Test



Fig. 1: Compressive strength test

The method to determine concrete cube compressive strength follows the standards set by IS: 516-1959. The compression testing machine received the specimen while ensuring that the load application avoided the cube sides corresponding to its casting arrangement by not applying stress to top or bottom faces. Fig. 1 demonstrates the variation of compressive strength. Compressive strength tests were carried out on a compression testing machine of 2000 kN capacity using the setup displayed in Fig 2. Table 6 contains the test results.

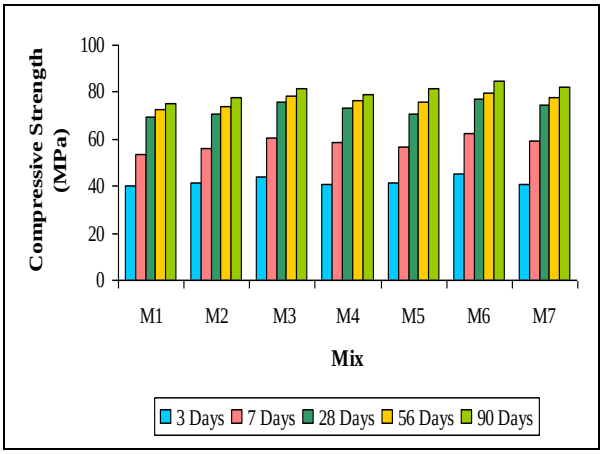


Fig. 2: Variation of compressive strength at various ages

The compressive strength of different mixes (M1–M7) was evaluated at 3, 7, 28, 56, and 90 days. The addition of silica fume significantly enhanced strength due to its high pozzolanic activity, forming more CSH gel. Mix M6 (7.5% SF, 0.2% GF) exhibited the highest 28-day strength of 77.33 MPa, while Mix M3 (7.5% SF) achieved 75.67 MPa, shown in Fig. 2. Strength gain is influenced by the silica fume content and curing age, with HPC showing higher strength than control specimens. The ultimate compressive strength was recorded when the cube cracked under load. Glass fiber provided a slight increase in compressive strength. Overall, the compressive strength improved with increasing concrete age.

3.2 Split Tensile Strength Test

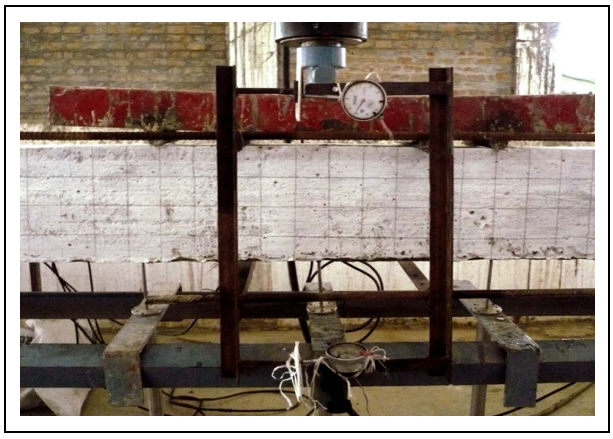


Fig. 3: Split tensile strength test

The method to obtain splitting tensile strength of concrete cylinders follows IS:5816-1999 standards. The testing system shall deliver an applied load at

nominal rate between 1.2 and 1.4. Table 7 shows the split tensile strength results.

Table 7. Split tensile strength result

Mix	SF (kg/m³)	Glass Fiber (kg/m³)	3 Days (MPa)	7 Days (MPa)	28 Days (MPa)	56 Days (MPa)	90 Days (MPa)
M1	0	0	40.33	53.67	69.33	72.67	75.33
M2	30	0	41.33	56.33	70.67	73.67	77.67
M3	45	0	43.67	60.33	75.67	78.33	81.33
M4	60	0	40.67	58.67	73.33	76.67	78.67
M5	30	1.2	41.67	56.67	70.67	75.67	81.33
M6	45	1.2	45.33	62.67	77.33	79.33	84.67
M7	60	1.2	40.67	59.33	74.67	77.67	82.43

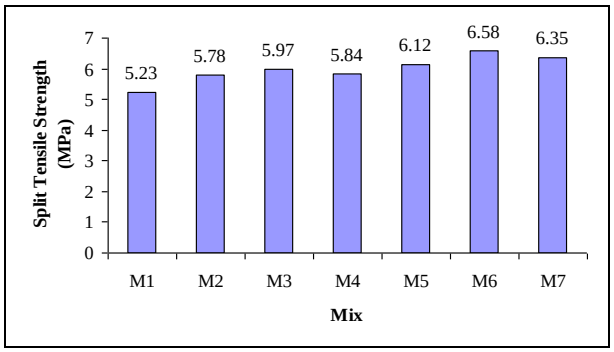


Fig. 4: Split tensile strength of various mixes

To assess the split tensile strength at 28 days, 100 x 200 mm cylinders were cast; the values ranged from 5.23 MPa to 6.58 MPa for various combinations. While Mix M6 (7.5% SF, 0.2% GF) reached the maximum strength of 6.58 MPa, Mix M3 (7.5% SF) had a greater split tensile strength. Compared to the control mix, M6's split tensile strength was 25.81% greater. Tensile strength increased by 10.52% for M2, 14.15% for M3, 11.66% for M4, 17.02% for M5, 25.81% for M6, and 21.41% for M7 in comparison to the control mix. The tendency was confirmed by the remarkable agreement between theoretical and experimental values. Fig. 3 and Fig. 4 illustrate how the split tensile strength varies across the various combinations.

3.3 Flexural Strength Test

The experimental procedure to determine concrete prism flexural strength follows the specifications of IS: 516-1959. The machine should be used to place the specimen with its load applied directly to the top surface as it was formed in the mould across two lines located 13.3 cm apart. A gradual load increment must be applied without abrupt force rises at 180 kg/min until the specimen fractures. The shortest distance which separates the fracture line from its nearest supporting element was detected. Table 8 shows the test results.



Fig. 5: Flexural strength test

Table 8. Flexural strength result

Mix	SF (kg/m³)	Glass Fiber (kg/m³)	28 Days (MPa)	Theoretical Value (MPa)
M1	0	0	5.43	5.83
M2	30	0	5.84	5.88
M3	45	0	6.05	6.09
M4	60	0	5.89	5.99
M5	30	1.2	6.33	5.88
M6	45	1.2	6.70	6.16
M7	60	1.2	6.54	6.05

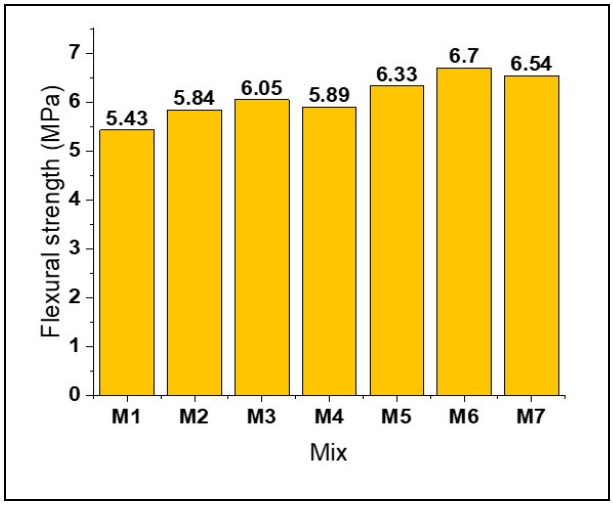


Fig. 6: Flexural strength of various mixes

Flexural strength at 28 days was measured using prisms, and it varied between 5.43 MPa and 6.70 MPa for the various combinations. With a flexural strength of 6.70 MPa, Mix M6 (7.5% SF, 0.2% GF) shown in Fig. 5, outperformed the control mix by 23.39%. Strength increases were 7.55% for M2, 11.42% for M3, 8.47% for M4, 16.57% for M5, 23.39% for M6, and 20.44% for M7 compared to the control mix. The findings were

validated by the near match between the experimental and theoretical values. Fig. 6 illustrates how the flexural strength varies for various mixtures.

3.4 Water Absorption Test

The ability of concrete cube to absorb water was evaluated in accordance with ASTM C 642-81 by first drying the specimens for 24 hours at 105 ℃, then submerging them in water until their weight remained constant. Absorption was calculated as the weight difference between the dry and saturated states. Table 9 shows the water absorption results.

Table 9. Water absorption result

Mix	SF (kg/m³)	Glass Fiber (kg/m³)	Wet weight of cube (gms)	Weight of cube in dry condition (gms)	In 24 Hrs Water Absorption (%)
M1	0	0	2625	2544	3.18
M2	30	0	2639	2561	3.05
M3	45	0	2645	2572	2.84
M4	60	0	2651	2583	2.63
M5	30	1.2	2699	2622	2.94
M6	45	1.2	2705	2635	2.66
M7	60	1.2	2765	2698	2.48

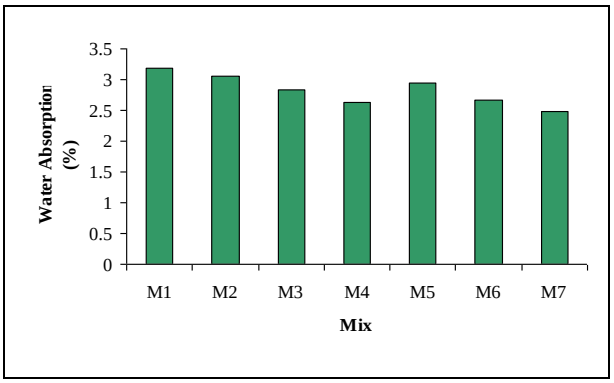


Fig. 7: Water absorption for various mixes

According to the findings of the water absorption test, the denser concrete matrix causes absorption to decrease as silica fume levels rise. M1 has the largest absorption (3.18%), whilst M7 has the lowest (2.48%), suggesting greater endurance. Higher silica fume concentration mixes have less porosity, which reduces water intrusion. By increasing concrete's density, mineral admixtures lower water absorption. The findings demonstrate that by reducing moisture penetration, a higher pozzolanic content improves durability (Fig. 7).

3.5 Modulus of Elasticity

The initial tangent modulus and secant modulus techniques are used to calculate the modulus of elasticity in concrete. At low stress levels, the initial tangent modulus is correct; at greater stress levels, it is not. Measured at different stress levels, such as 15%, 25%, or 33% of the ultimate strength, the secant modulus is often employed in practice. Using uniaxial compression experiments, the modulus is computed from stress-strain data with a Young's modulus of 51,899.03 N/mm^2, M3 exhibits the maximum rigidity among the blends. M7 has the lowest value at 41,613.58 N/mm^2. The findings verify that silica fume raises the modulus of elasticity, which improves the overall performance of the concrete. The model calculaton to determine the modulus of elasticity is given below.

3.5.1 Steps to calculate the Modulus of Elasticity

In the first step data points are extracted form the stress-strain curve. Then identify the linear portion of the curve which is elastic. Then fit a straight line to determine the slope. Then calclute the modulus of elasticity using the formula as follows:

$$\text{Modulus of elasticity(E)} = \frac{\Delta\sigma}{\Delta\varepsilon}$$

$\mathbf{\Delta\sigma}$ = Change in stress
$\mathbf{\Delta\varepsilon}$ = Change in strain

Model calculation:

Extracting data points from the curve(Fig. 8) and calculate Young's modulus based on the initial linear portion of the curve. The edges of the stress-strain curve have been extracted. Then the key data points are identified from the linear elastic region and then finally Young's modulus has been calculated using the slope of that section. From the Fig. 8 , Two points in the linear elastic region has been visualized and then noted as follows.

Point 1: (Strain = 200×10^{-6}, Stress = 10.5 MPa)
Point 2: (Strain = 800×10^{-6}, Stress = 41.639 MPa)

$$\text{Modulus of elasticity(E)} = \frac{\Delta\sigma}{\Delta\varepsilon}$$

$$\text{Modulus of Elasticity} = \frac{(41.639-10.500)}{(800-200)\times 10^{-6}}$$

$$= 51899.03 \text{ N/mm}^2$$

3. 6 Stress-strain Behavior

A 2000 kN capacity machine was used to perform compression tests on 100×200 mm cylinder specimens in order to examine the stress-strain behaviour of HPC. Throughout the test, axial stress and strain values were recorded at regular intervals. Fig. 8 shows the stress-strain curves for mixtures M1 to M7. The findings show that M3, which contains 7.5% silica fume,

has greater strength and ultimate strain than regular concrete. Table 10 provides a summary of the maximum stress and strain values for each blend.

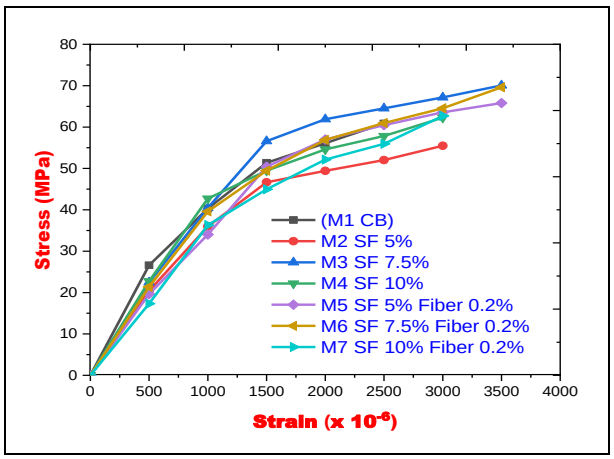


Fig. 8: stress-strain curves for various mixes

Table 10. Maximum stress strain values

Mix	Stress (MPa)	Strain
M1	61.52	2480
M2	57.23	3150
M3	71.16	3370
M4	64.68	3185
M5	68.24	3320
M6	72.34	3530
M7	63.42	3215

3.7 Preparation of Beam Specimens

The structural laboratory was used to cast high-performance geopolymer concrete beams with different silica fume and glass fibre contents. Before the concrete was poured, wooden moulds were prepared and greased, and a rotary mixer was used to combine the raw components. Stirrups were used to secure the cut reinforcement bars, and binding wires were used to ensure adequate spacing. The concrete was mixed for 3 to 5 minutes, then put into moulds, demoulded 24 hours later, and allowed to cure for 28 days using gunny bags. After the curing time, beams were cleaned with sandpaper to get rid of grit and allowed to dry for a full day. All specimens were whitewashed to improve the visibility of cracks during testing. The flexural behaviour of these beams, including moment-curvature, deflection, and load-bearing capability, was then assessed by two-point loading tests.

3.8 Experimental Test Setup for Beam Specimens

One traditional reinforced concrete beam and six beams with different silica fume replacements of 5%, 7.5%, and 10% were among the seven high-performance geopolymer concrete beams that were produced. Only SF was present in three of these beams, while SF and 0.2% glass fibre reinforcement were present in the other three. Using a 1000 kN capacity frame on a 1500 mm effective span under simply supported circumstances, all beams were tested under two-point loads. With the use of linear variable differential transducers (LVDTs), deflections were monitored at mid-span and loading locations. At every load increase, crack patterns were noted, and testing was carried out until failure. A curvature meter with a dial gauge arrangement was used to measure strain. According to the experimental findings, SF and glass fibre improved flexural performance, enhancing ductility. Table 11 shows the test results for the flexure beam.

Table 11. Test results for flexure beam

Specimens	SF (kg/m³)	Glass Fiber (kg/m³)	First Crack Load (kN)	Ultimate load (kN)	Deflection at Ultimate Load (mm)
M1	0	0	26	46	12.46
M2	30	0	28	48	14.65
M3	45	0	32	54	17.75
M4	60	0	30	52	16.26
M5	30	1.2	35	52	17.89
M6	45	1.2	38	58	21.77
M7	60	1.2	37	54	19.08

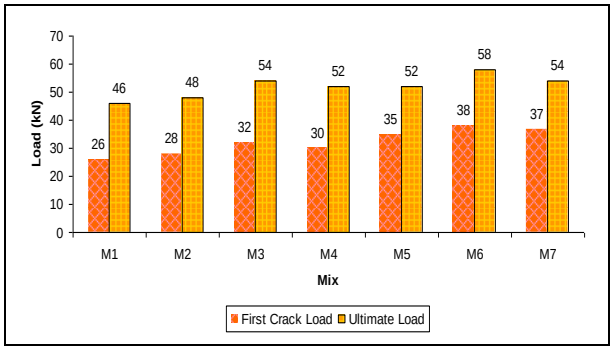


Fig. 9: Comparison for first crack load and ultimate load

Figure 9 presents a comparison of the first crack load and the ultimate load. The load deflection curves for flexural beams from M1 to M7 is plotted in the Figure 10. The load-deflection curve of M1 rises steeply from the beginning before showing elastic conduct. The point of initial cracking occurs at 26 kN resulting in a brittle failure when reaching 48 kN before deflection hits 12.46 mm, which indicates low ductility. M2 exhibits first crack strength of 28 kN and reaches ultimate strength at 48 kN (M2 - 30 kg/m³ SF). The deflection reached 14.65 mm in M2, whereas M1 experienced less ductility and energy absorption at a lower 12.46 mm deflection value. M3 extends the first crack load to 32 kN before reaching its ultimate load of 54 kN while achieving a deflection of 17.75 mm. The gradual bending shape of the curve

during failure testifies to better load distribution and improved toughness of the material M4 demonstrates first crack strength at 30 kN together with an ultimate strength at 52 kN while reaching high deflection at 16.26 mm. An excess of granular material in concrete has the effect of reducing strength slightly, but it allows ductility to improve M5 mixture which contains 30 kg/m³ SF and 1.2 kg/m³ glass fiber shows enhanced first crack strength of 35 kN and ultimate strength of 52 kN, achieving 17.89 mm deflection. Glass fibers added to concrete create enhanced capacity to extend beyond the initial cracking point, hence increasing material ductility

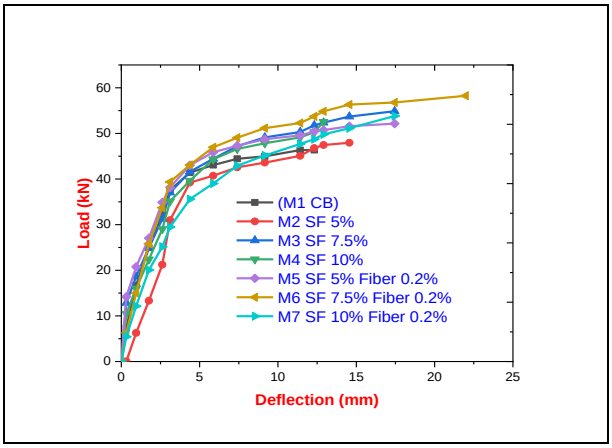


Fig. 10: Load-Deflection curves for flexural beams

The first crack load (38 kN) and ultimate load (58 kN) reach maximum values in M6, while the deflection attains its maximum at 21.77 mm. The curve shows excellent toughness because glass fibers act as bridging elements that halt sudden failure during cracks. M7 exhibits a slightly reduced first crack load (37 kN) and ultimate load (54 kN) compared to M6, but with good deflection (19.08 mm). The curve suggests that while the combination of SF and glass fiber improves performance, excessive SF may slightly reduce peak strength

3.9 Beam Test

The flexural test results indicate that the M6 beam, with 7.5% silica fume and 0.2% glass fiber, achieved the highest ultimate load capacity of 58 kN, which is 26.08% higher than the control beam (M1). The first crack appeared at 26 kN for M1, whereas M3 exhibited a first crack load of 32 kN, showing a 23.07% improvement. The ultimate load of M3 was 54 kN, 17% higher than M1. Experimental results showed that ultimate load capacities exceeded theoretical values.

From the moment-curvature relationship, beams with 5% silica fume exhibited higher stiffness in the elastic stage, while 7.5% SF beams (M3) demonstrated superior ductility in the plastic stage. The inclusion of fibers further enhanced the load-carrying capacity, with M6 showing a 7.41% increase over M3. The curvature and rotation ductility were significantly improved in beams with 7.5% silica fume.

SEM analysis of M1 revealed a thick geopolymer matrix with visible pores and unreacted fly ash or GGBS particles, indicating partial geopolymerization. The presence of fibrous structures and microcracks suggested the role of alkaline activation in binding the constituents. This microstructural development contributes to improved mechanical properties, crucial for enhancing flexural performance.

3.10 SEM Analysis of Specimen

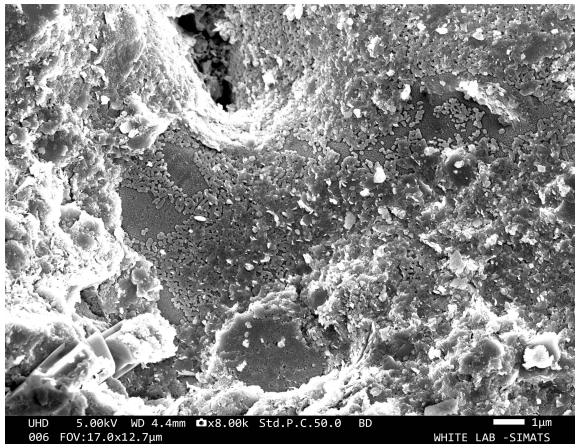


Fig. 11: SEM analysis of specimen M1

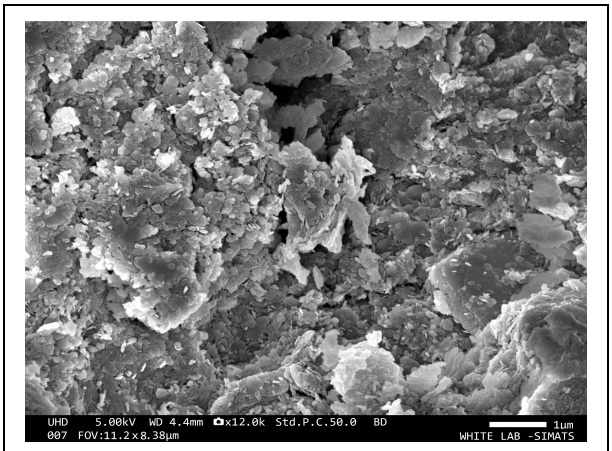


Fig. 12: SEM analysis of specimen M5

The microstructural properties of high-performance geopolymer concrete without silica fume replacement are shown in SEM analysis of specimen M1 in Fig. 11. Partial geopolymerization is indicated by the thick geopolymer matrix development in the image, which includes some visible pores and unreacted fly ash or GGBS particles. The existence of fibrous structures and micro cracks indicates that alkaline activation plays a part in binding the constituent parts of the mix. This

morphology demonstrates how geopolymerization improves mechanical qualities, which are essential for flexural performance.

The SEM image of sample M5 illustrates the microstructural development of high-performance geopolymer concrete with 7.5% silica fume replacement. A denser matrix with reduced porosity is evident, indicating enhanced geopolymerization and better particle packing. The image shows fewer unreacted fly ash or GGBS particles, confirming improved binding due to silica fume addition. This refined microstructure contributes to increased compressive strength and improved flexural performance in geopolymer concrete. Fig. 12 shows the SEM analysis of specimen M5.

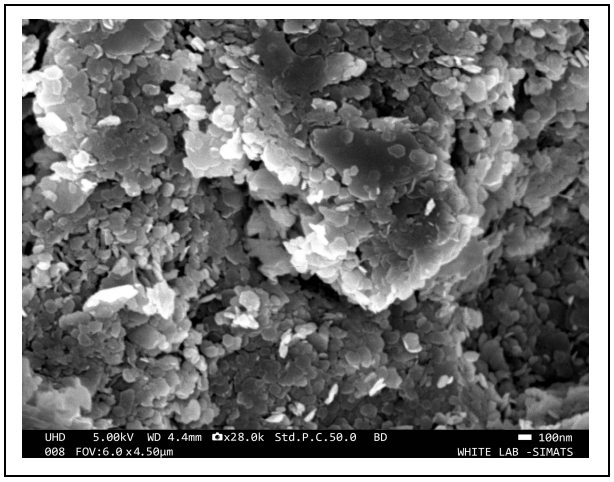


Fig. 13: SEM analysis of specimen M7

The microstructural characteristics of high-performance geopolymer concrete with 10% silica fume substitution are shown in Fig. 13. SEM analysis of specimen M7. Better bonding and increased geopolymerization are suggested by the tight, compact matrix with fewer apparent pores. Higher compressive strength results from improved particle packing, which is shown by the existence of tiny particles that are evenly distributed. By supporting enhanced flexural and tensile capabilities, this finely tuned microstructure maximises the performance of the concrete.

3.11 XRD Analysis of Specimen

With 84.8% amorphous content and 15.2% crystalline phases, sample M1's XRD examination shows a mostly amorphous geopolymer structure. The existence of an aluminosilicate gel, which gives geopolymer concrete its binding qualities, is confirmed by the wide hump in the diffraction pattern. Partial geopolymerization is suggested by the crystalline peaks, which match unreacted fly ash or GGBS particles. The enhanced mechanical performance shown in high-performance geopolymer concrete is a result of this amorphous-dominated structure shown in Fig. 14.

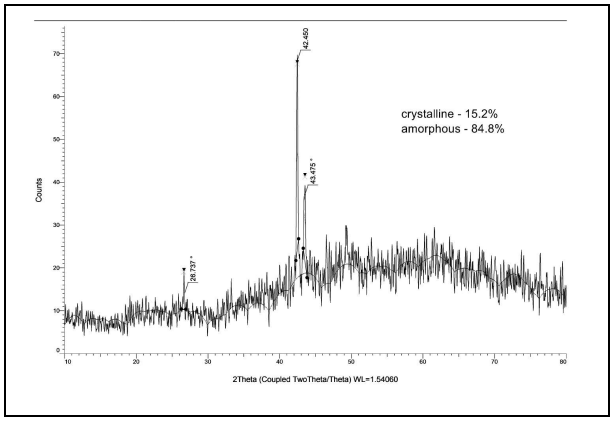


Fig. 14: XRD analysis of specimen M1

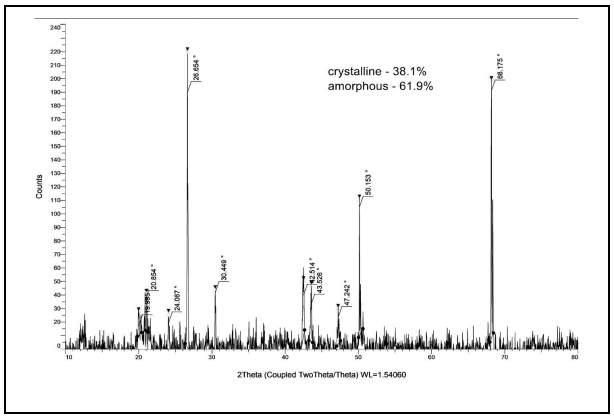


Fig. 15: XRD analysis of specimen M5

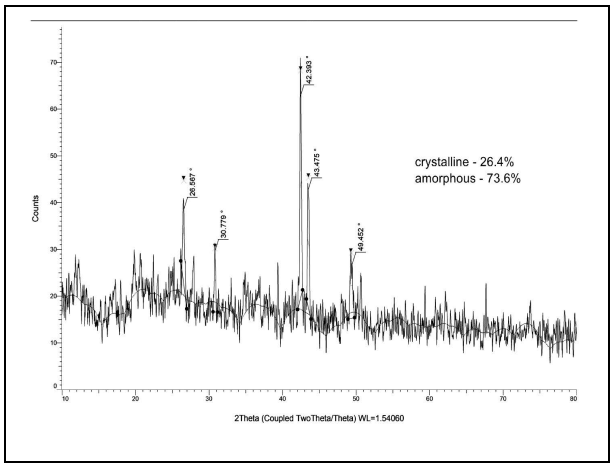


Fig. 16: XRD analysis of specimen M7

The XRD examination of sample M5 (Fig. 15) reveals a decreased amorphous content of 61.9% and an increased crystalline phase of 38.1%, suggesting improved geopolymerization as a result of silica fume substitution. Sharper crystalline peaks are indicative of greater reaction product production, which enhances mechanical characteristics. Increased strength results from the conversion of raw materials into stable crystalline phases, which is shown by the decrease in

amorphous content. The enhanced compressive and flexural behaviour of the geopolymer concrete is supported by this structural improvement.

Fig. 16 shows the XRD pattern of sample M7, which comprises of moderately developed geopolymeric matrix with a crystalline phase of 26.4% and an amorphous component of 73.6%. The existence of unreacted or partly reacted silica and alumina is suggested by the increased amorphous phase, which might impact the overall densification of the material. The comparatively smaller crystalline peaks suggest a less comprehensive development of reaction products in comparison to other mixtures, which may have an impact on strength properties. The results that silica fume replacement at 7.5% maximises compressive strength and enhances the mechanical performance of geopolymer concrete are consistent with this structural composition.

4. CONCLUSION

The highest 28-day compressive strength was achieved by Mix M6 (77.33 MPa), showing a 25.81% increase over the control mix due to silica fume's pozzolanic activity and improved CSH gel formation. Mix M6 showed the highest split tensile strength (6.58 MPa), with a 25.81% improvement over the control mix, confirming the beneficial effects of glass fibres with silica fume. The highest 28-day flexural strength (6.70 MPa) was recorded for Mix M6, marking a 23.39% increase over the control mix, showing that silica fume and fibers enhance tensile load resistance. The lowest absorption (2.48%) was observed in Mix M7, indicating a denser concrete matrix with lower porosity due to increased silica fume content. Mix M3 recorded the highest Young's modulus (51,899.03 N/mm²), suggesting that silica fume enhances concrete stiffness and rigidity. Mix M6 achieved the highest ultimate load (58 kN), showing a 26.08% increase over the control beam, while silica fume improved ductility and load-carrying capacity. SEM images confirmed denser microstructures with silica fume, reducing porosity and unreacted particles, while XRD analysis showed a high percentage of amorphous aluminosilicate gel, contributing to superior mechanical properties. It is concluded that mix M6 is the best mix considering both compressive strength and flexural strength.

FUNDING

This research received no specific grant from any funding agency in the public, commercial, or not-for-profit sectors.

CONFLICTS OF INTEREST

The authors declare that there is no conflict of interest.

COPYRIGHT

This article is an open-access article distributed under the terms and conditions of the Creative Commons Attribution (CC BY) license (http://creativecommons.org/licenses/by/4.0/).

REFERENCE

Abdellatief, M., Alanazi, H., Radwan, M. K. H. and Tahwia, A. M., Multiscale Characterization at Early Ages of Ultra-High Performance Geopolymer Concrete, *Polym*., 14(24), 5504(2022). https://doi.org/10.3390/polym14245504

Amin, M. N., Khan, K., Javed, M. F., Aslam, F., Qadir, M. G. and Faraz, M. I., Prediction of Mechanical Properties of Fly-Ash/Slag-Based Geopolymer Concrete Using Ensemble and Non-Ensemble Machine-Learning Techniques, *Mater*., 15(10), 3478(2022). https://doi.org/10.3390/ma15103478

Hawarneh, A. A., Aldabagh, S. and Alam, M. S., Experimental Investigation on Compressive, Tensile, and Flexural Strengths of Concrete with High Volume of GGBS, Fly Ash, and Silica Fume, *Proc. Can. Soc. Civ. Eng. Annu. Conf*., 367, 805–824(2024). https://doi.org/10.1007/978-3-031-35471-7_57

Nagajothi, S., Elavenil, S., Angalaeswari, S., Natrayan, L. and Mammo, W. D., Durability Studies on Fly Ash Based Geopolymer Concrete Incorporated with Slag and Alkali Solutions, *Adv. Civ. Eng*., 2022(1), 7196446(2022). https://doi.org/10.1155/2022/7196446

Prakash, S., Kumar, S., Biswas, R. and Rai, B., Influence of silica fume and ground granulated blast furnace slag on the engineering properties of ultra-high-performance concrete, *Innovative Infrastruct. Solutions*, 7(1), 117(2022). https://doi.org/10.1007/s41062-021-00714-7

Rambabu, D., Sharma, S. K. and Akbar, M. A., Fatigue analysis of ambient-cured geopolymer concrete for high-traffic pavements, *Environ. Sci. Pollut. Res*., x, xx(2024). https://doi.org/10.1007/s11356-024-34402-7

Saini, K., Matsagar, V. A. and Kodur, V. R., Recent advances in the use of natural fibers in civil engineering structures, *Constr. Build. Mater*., 411, 134364(2024). https://doi.org/10.1016/j.conbuildmat.2023.134364

Sujitha, V. S., Ramesh, B. and Xavier, J. R., Investigation of functionalized graphene oxide incorporated superabsorbent polymers for enhanced durability, hydration, microstructure and mechanical strength of modified concrete, *Compos. Interfaces*, 38(2)1–38(2024a). https://doi.org/10.1080/09276440.2024.2407249

Sujitha, V. S., Ramesh, B. and Xavier, J. R. Investigation of Bi-functionalized Clay-Superabsorbent Polymer Nanocomposite for Improved Mechanical and Durability Properties of Cementitious Materials, *Arab. J. Sci. Eng*., 49(9), (2024b), https://doi.org/10.1007/s13369-024-09525-1

Suresh, K. A., Muthukannan, M., Arunkumar, K., Chithambar, G. A. and Kanniga, D. R., Utilisation of waste glass powder to improve the performance of hazardous incinerated biomedical waste ash geopolymer concrete, *Innovative Infrastruct. Solutions*, 7(1), 93(2022). https://doi.org/10.1007/s41062-021-00694-8

Swathi, B and Vidjeapriya, R., Influence of precursor materials and molar ratios on normal, high, and ultra-high performance geopolymer concrete – A state of art review, *Constr. Build. Mater*., 392, 132006(2023). https://doi.org/10.1016/j.conbuildmat.2023.132006

Tashan, J., Flexural behavior evaluation of repaired high strength geopolymer concrete, *Compos. Struc*., 300, 116144(2022). https://doi.org/10.1016/j.compstruct.2022.116144

Thakur, G., Singh, Y., Singh, R., Prakash, C., Saxena, K. K., Pramanik, A., Basak, A. and Subramaniam, S., Development of GGBS-Based Geopolymer Concrete Incorporated with Polypropylene Fibers as Sustainable Materials, *Sustainability*, 14(17), 10639(2022). https://doi.org/10.3390/su141710639

Xie, J., Zhao, J., Wang, J., Wang, C., Huang, P. and Fang, C., Sulfate Resistance of Recycled Aggregate Concrete with GGBS and Fly Ash-Based Geopolymer, *Mater.*, 12(8), 1247(2019). https://doi.org/10.3390/ma12081247